Permafrost Degradation Diminishes Terrestrial Ecosystem Carbon Sequestration Capacity on the Qinghai-Tibetan Plateau

Lei Liu[1,2,3], Qianlai Zhuang[3], Dongsheng Zhao[1], Du Zheng[1,2], Dan Kou[3,4], Yuanhe Yang[2,5]

[1]Key Laboratory of Land Surface Pattern and Simulation, Institute of Geographical Sciences and Natural Resources Research, Chinese Academy of Sciences, Beijing 100101, China.

[2]University of Chinese Academy of Sciences, Beijing 100049, China.

[3]Department of Earth, Atmospheric, and Planetary Sciences, Purdue University, West Lafayette, IN 47907, USA

[4]Biogeochemistry Research Group, Department of Biological and Environmental Sciences, University of Eastern Finland, Kuopio, Finland

[5]State Key Laboratory of Vegetation and Environmental Change, Institute of Botany, Chinese Academy of Sciences, Beijing 100093, China

Corresponding author: Dongsheng Zhao (zhaods@igsnrr.ac.cn)

Key Points:

- Soil carbon release due to permafrost degradation overwhelms net primary production on the Qinghai-Tibetan Plateau.
- Deep soil nitrogen addition from thawing permafrost has a limited benefit to plant carbon uptake.
- Permafrost degradation has more pronounced influence on carbon cycling of alpine meadow than alpine steppe.

Abstract

Effects of permafrost degradation on carbon and nitrogen cycling on the Qinghai-Tibetan Plateau (QTP) have rarely been analyzed. This study used a revised process-based biogeochemical model to quantify the effects in the region during the 21st century. We found that permafrost degradation would expose 0.98±0.49 (mean±SD) and 2.17±0.38 Pg C of soil organic carbon under the representative concentration pathway (RCP) 4.5 and the RCP 8.5, respectively. Among them about 60% will be decomposed, enhancing heterotrophic respiration by 9.54±5.20 (RCP 4.5) and 38.72±17.49 (RCP 8.5) Tg C/yr in 2099. Deep soil nitrogen (N) supply due to thawing permafrost is not accessible to plants, providing limited benefits to plant growth and only stimulating net primary production by 6.95±5.28 (RCP 4.5) and 27.97±12.82 (RCP 8.5) Tg C/yr in 2099. As a result, permafrost degradation would weaken the regional carbon sink (net ecosystem production) by 303.55±254.80 (RCP 4.5) and 518.43±234.04 (RCP 8.5) Tg C cumulatively during 2020–2099. Permafrost degradation has a higher influence on C balance of alpine meadow than alpine steppe ecosystems on the QTP. The shallower active layer, higher soil C and N stocks, and wetter environment in alpine meadow are responsible for its stronger response of C balance to permafrost thaw. This study highlights that permafrost degradation could continue to release large amounts of carbon to the atmosphere irrespective of potentially more nitrogen available from deep soils.

1 Introduction

Permafrost degradation due to climate warming makes large amounts of frozen soil organic matter (SOM) available for decomposition, leading to a positive feedback to the climate system by releasing greenhouse gases (GHG) (Koven et al., 2011; Koven, Schuur et al., 2015; Schaefer et al., 2014; Schuur et al., 2015). Enhanced decomposition in permafrost regions also increases nutrient availability however (Keuper et al., 2012; Salmon et al., 2016, 2018), stimulating plant production together with the effects of increasing air temperature, expanding growing season, shifting plant community composition, and rising atmospheric CO_2 concentration, resulting in a negative feedback to climate warming (Finger et al., 2016; Liang et al., 2018; Peng, X. et al., 2020; Zhuang et al., 2010). Considerable uncertainty of these positive and negative feedbacks limits our ability to model C balance of the permafrost region (Abbott et al., 2016).

Coupling the impact of permafrost degradation into land surface models has projected that the northern high latitudes would shift from a net C sink (Qian et al., 2010) to a net source to the atmosphere (Burke et al., 2013; Koven et al., 2011; MacDougall et al., 2016; Schaefer et al., 2014; Schaphoff et al., 2013). However, large uncertainties still exist in the magnitude of the estimated changes in soil, vegetation, and ecosystem C stocks (McGuire et al., 2016). Model structural differences, particularly in the soil carbon decomposition processes, have been attributed to be the largest uncertainty in quantifying permafrost carbon-climate feedbacks (Burke et al., 2017).

A critical model structural feature to represent the permafrost carbon-climate feedback is to consider soil C exposure with thaw depth (McGuire et al., 2018). In permafrost regions, part of soil organic carbon (SOC) is protected from decomposition by frozen soil but may become more susceptible to decomposition with warming-induced degradation of permafrost. To better account for the influence of permafrost dynamics on terrestrial carbon balance, soil C exposure due to thawing permafrost should be incorporated into land surface models. Hayes et al. (2014)

assessed the net effect of active layer dynamics on permafrost carbon feedback during 1970–2006 over the circumpolar permafrost region and found that permafrost degradation exposed 11.6 Pg C of thawed SOM to decomposition, resulting in 4.03 Pg C releasing from the decomposition of newly exposed SOM, but only 0.3 Pg C was compensated by net primary production (NPP). Using a carbon-nitrogen model that includes permafrost processes and depth-dependent changes in SOM, Koven et al. (2015a) found similar results and projected that permafrost carbon-climate feedback is sensitive to deep soil carbon decomposability, and the impact of deep soil nitrogen (N) mineralization on C budget is small. However, projections of five biogeochemical models that represent soil C explicitly with depth show that the northern permafrost region would likely act as a net C sink before 2100 due to stronger vegetation C uptake (McGuire et al., 2018). The different result found by McGuire et al. (2018) maybe because they only considered the active layer thickness (ALT) less than three meters. The decomposition of large quantities of deep carbon deposits (Schuur et al., 2015) may reverse this estimation.

The Qinghai-Tibetan Plateau (QTP) is characterized by a deep ALT (2.34±0.70 m), and about 15% of the QTP permafrost region has ALT greater than 3 m (Wang, T. et al., 2020). SOC storage on the QTP is estimated at 50.43 Pg, of which 35.10 Pg stores below 3 m soils and 37.21 Pg frozen in permafrost currently (Wang, T. et al., 2020). Based on the vertical distribution of SOC and the change of ALT, Wang, T. et al. (2020) estimated that permafrost thaw on the QTP would expose 1.86±0.49 and 3.80±0.76 Pg frozen C to decomposition, which could potentially turn the region from a net C sink to a net source. The lack of the simulation of SOM decomposition, and the use of net biome production (NBP) from CMIP5 models (which did not consider permafrost carbon (Jones et al., 2016) and hence the stimulation of N supply to vegetation production due to permafrost thaw), may bias the estimation of net C budget of Wang, T. et al. (2020). Through repeated soil carbon measurements on the QTP, Ding et al. (2017) suggested that the upper active layer of the QTP permafrost currently represents a substantial regional soil C sink, probably owing to enhanced vegetation growth. However, this study only examined SOC stocks in uppermost 30 cm. Carbon changes associated with deeper and older permafrost remain largely unknown (Mu et al., 2020). Inadequate studies that focus on representing soil C explicitly with depth, particularly representing soil C in deep soils, and simultaneously consider the feedback of vegetation to permafrost thaw impedes our understanding of permafrost carbon-climate feedbacks on the QTP.

Apart from deep ALT, the environment of the permafrost regions on the QTP is also different from the pan-Arctic in water condition. Specifically, annual precipitation decreases from southeastern to northwestern on the QTP. As a result, the eastern QTP receives more precipitation and dominated by alpine meadow ecosystem, while the widespread inner and western parts are controlled by alpine dry climate and dominated by alpine steppe ecosystems. Many studies have found that the alpine steppe and alpine meadow ecosystems respond differently to climate change (Hao et al., 2021; Li, S. et al., 2019; Liu et al., 2020; Peng, F. et al., 2020). For example, warming experiment revealed that warming increased plant productivity in alpine meadow but decreased productivity in alpine steppe (Ganjurjav et al., 2016). Temperature sensitivity of ecosystem respiration (Q10) in alpine meadow (3.4) can be twice the number in alpine steppe (1.7) (Wang, L. et al., 2018). The distinct environment and the different responses to climate change of these two ecosystems could result in different permafrost C feedbacks. However, currently the effects of active layer deepening on C balance of these two ecosystems are still not certain.

In this study, a process-based biogeochemical model was revised by coupling thaw depth with soil C exposure to analyze the following issues: (*i*) the quantity of frozen SOC in deep soils on the QTP that will be exposed to decomposition due to permafrost thaw in the 21st century, and the quantity of C that will be released into the atmosphere; (*ii*) the stimulation of deep permafrost thaw on vegetation productivity due to extra N supply and the net effect of permafrost thaw on ecosystem C balance (enhanced heterotrophic respiration (RH) versus stimulated net primary production (NPP)); and (*iii*) the different responses of C balance of the distinct alpine meadow and alpine steppe to permafrost thaw.

2 Methods and Data

2.1 The Terrestrial Ecosystem Model

The Terrestrial Ecosystem Model (TEM) is a process-based, global scale biogeochemical model, using spatially explicit soil, vegetation, and elevation data and climate forcing of radiation, precipitation, and air temperature data to simulate ecosystem C and N cycling (McGuire et al., 1992; Zhuang et al., 2002). A soil thermal model (STM) has been coupled into TEM to represent vertical soil thermal profile in permafrost- and non-permafrost-dominated ecosystems and gives TEM the ability to describe freeze-thaw cycles in cold regions (Jin et al., 2015; Zhuang et al., 2001, 2010). The effects of freeze-thaw dynamics on gross primary production (GPP) have also been considered in TEM (Zhuang et al., 2011). TEM has been extensively used to evaluate C dynamics in northern high latitudes and Tibet plateau (e.g., Hayes et al., 2014; Jin et al., 2013, 2015; Kicklighter et al., 2019; McGuire et al., 2018).

In previous versions of TEM, soil organic carbon (SOC) in the entire root zone is assumed to be available for decomposition, and thus take part in heterotrophic respiration. However, since active layer thicknesses (ALT) in permafrost regions are often shallower than root depth defined in TEM (Hayes et al., 2011, 2014), part of SOC in root zone is frozen in soil and protected from microbial decomposition. Therefore, SOC considered in heterotrophic respiration quantification is smaller than the entire SOC stock in root zone. TEM6 (Hayes et al., 2011, 2014) has considered the amount of SOC available for decomposition and treated it as a proportion the entire root zone SOC, depending upon the ratio of ALT to rooting depth. By calculating ALT variation over time through the STM module in TEM, this approach has been used to estimate the potential influence of permafrost thaw on the availability of soil organic matter to decomposition (Hayes et al., 2014; Kicklighter et al., 2019). However, this approach did not consider SOC below the rooting zone and assumed that they do not contribute to C flux. When warming continues in the future and ALT deepens below rooting depth, this approach may underestimate the influence of permafrost degradation on the availability of carbon to decomposition (Hayes et al., 2011).

On the QTP, ALT (2.34 m; Wang, T. et al., 2020) is usually much deeper than rooting depth (over 90% of plant roots are distributed within the top 30 cm soil layer; Yang, Y. et al., 2009). Future permafrost degradation would probably happen far below rooting zone. Therefore, we modified the approach by adjusting SOC according to the ratio of ALT of current time step to previous time step, rather than the ratio of ALT to rooting zone depth:

$$SOC_i = SOC_{i-1} * \left(1 + \frac{prop_i - prop_{i-1}}{prop_{i-1}}\right) \quad (1)$$

$$prop_i = \frac{a * ALT_i}{b + ALT_i} \tag{2}$$

where i and i-1 denote the current and previous year, respectively; ALT_i is the maximum ALT of the current year; $prop_i$ denotes the proportion of SOC in the active layer of current year to the total SOC in the entire soil profile. The hyperbolic function of $prop_i$ describes the vertical distribution of SOC in soil profile, with high density of SOC in shallow soil layers but decreases towards deep soil, as documented by Hayes et al. (2014). a and b are parameters controlling the shape of the curve that how SOC density changes with soil depth. We estimated parameter b for alpine meadow, alpine steppe, and alpine desert using observation data (Figure S1). For the remaining ecosystems, we set parameters b according to Kicklighter et al. (2019). Parameter values of b for various ecosystems are listed in Table S1. Parameter a will be divided when put eq. (2) into eq. (1).

Using this method, SOC within the soil layers that permafrost degraded was factored into total available SOC pools for soil decomposition. Although we considered the fact that SOC density decreases with soil depth, the vertical variations in SOC turnover time are still missing in this study, which may overestimate SOC decomposition rate to some extent (Shu et al., 2020).

Permafrost degradation influences not only the amount of SOC, but also soil organic N (SON), available inorganic N (AVALN), and soil water content. These variables were also adjusted according to the variation of ALT, in the same method as that for SOC. Although permafrost degradation can increase AVALN pools, if ALT deepens far below rooting depth, we assume that the additional AVALN cannot be accessed by vegetation. Therefore, only AVALN in rooting zone was used for vegetation N uptake (VegNup) calculation when ALT is greater than rooting zone depth.

Two freezing fronts are modeled in TEM, including freezing down due to cold air temperature and freezing up due to permafrost underneath the soils (Zhuang et al., 2001). ALT in permafrost regions is calculated as the total depth of unfrozen soil layers above the two freezing fronts. TEM does not explicitly 'define' permafrost occurrence in a grid cell, but infer its depth based on the 0 °C isotherm in the soil thermal profile. The permafrost region of this study was derived from permafrost map of China (Wang, 2019).

2.2 Model calibration and validation

TEM has been calibrated for terrestrial ecosystems on the QTP by Zhuang et al. (2010) and Jin et al. (2013, 2015). In this study, some key rate-limiting parameters (such as the maximum rate of photosynthesis, heterotrophic respiration, and plant N uptake and respiration rate) were recalibrated for three major ecosystems (i.e., alpine shrubland, alpine meadow, and alpine steppe), which occupy 82.6% of the permafrost regions on the plateau according to the 1:1000000 vegetation map of China (Figure 1; Chinese Academy of Sciences, 2001). The parameters were optimized by minimizing the differences between observations and simulations through altering parameters and iterating model simulations. The rest of the model parameters were set as previous studies. Site information of these three ecosystems is provided in Table S2. Observations of soil temperature (DST), net ecosystem production (NEP), and soil C and N stocks for each site are derived from references in Table S2 accordingly. The model was validated with 289 observations of soil C and N pools (data derived from Ding et al. (2016), Kou et al. (2019), and Wang et al. (2020)) on the plateau. These observation sites spread over alpine desert, alpine steppe, alpine meadow, and alpine cushion ecosystems. However, for the analysis of the effects of permafrost degradation, only the dominant ecosystems of alpine steppe and alpine meadow were focused on.

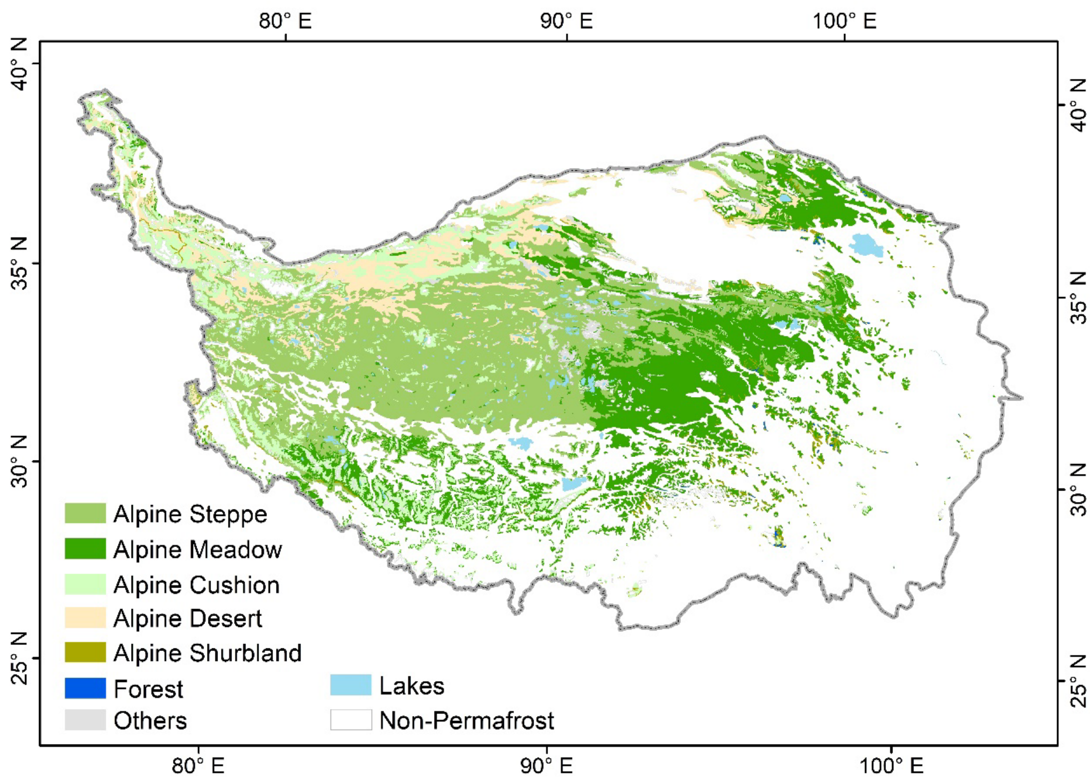

Figure 1. Vegetation distribution in the permafrost regions of the QTP. The vegetation distribution was derived from a 1:1,000,000 vegetation map of China (Editorial Committee of Vegetation Map of China, Chinese Academy of Sciences, 2001) provided by the Resources and Environment Science Data Center, Chinese Academy of Sciences. The permafrost map (all the colored patches exclude lakes) was obtained from frozen ground map of China (Wang, T., 2019).

2.3 Simulation protocol

To determine the direct effects of ALT deepening on ecosystem C dynamics, we carried out two simulations: the referenced simulation (S_R) and the transient simulation (S_T). The two simulations share the same model inputs but have differences in model structure. They are identical until 2020. After that, ALT changes with climate in S_T but remained no change in S_R. Therefore, C and N pools do not change with ALT in S_R after 2020 but does influenced by ALT in S_T. Through comparing the results of these two simulations, the direct effects of ALT changes on ecosystem C dynamics can be estimated.

TEM was spun up for 200 years in both simulations. During the spin-up procedure, climate data from 2006 to 2046 were used to force the model run and repeated continuously until dynamic equilibrium was achieved. The state variables of the dynamic equilibrium were then used as the initial value for simulations from 2006 to 2099. The spin-up procedures were identical for the S_R and S_T.

2.4 Data

TEM was driven with spatially referenced information on climate, soils, vegetation, and elevation for spatial extrapolation.

Climate data from 2006 to 2099 include air temperature (°C), precipitation (mm), and incident short-wave solar radiation (W/m^2), deriving from four global circulation models (GCMs: IPSL-CM5A-LR, GFDL-ESM2M, MIROC5, and HadGEM2-ES) in the second simulation round of the Inter-Sectoral Impact Model Intercomparison Project (ISI-MIP 2b). Known issues of previous round of ISIMIP have been solved for the ISIMIP2b through a series of adjustments, and atmospheric data provided by the ISIMIP2b have also been bias-adjusted to a new reference dataset of EWEMBI (Frieler et al., 2017). Regional simulation of this century was conducted under two climate scenarios of the Representative Concentration Pathway 4.5 (RCP 4.5) and RCP 8.5, which correspond to radiative forcing levels of 4.5 and 8.5 W/m^2 by 2100, respectively (Moss et al., 2010).

Soil texture data over the QTP were based on the Regridded Harmonized World Soil Database v 1.2 (Wieder, 2014). Vegetation and elevation data were derived from the 1:1000000 vegetation map of China (Chinese Academy of Sciences, 2001) and the Shuttle Radar Topography Mission (SRTM; Farr et al., 2007), respectively.

The spatial resolutions of soil texture and elevation data are 0.05 degree and 90 m, respectively. Compared with these land surface datasets, the climate data are much coarser, at the spatial resolution of 0.5 degree. On the QTP, topography, vegetation and soil may change greatly within 0.5-degree spatial resolution. To consider the effects of heterogeneities of these data, we resampled them into a spatial resolution of 0.1 degree. During resampling, we make every 25 grids of the resampled climate data share the same value as the grid of the same location of the original climate data. We did not adjust climate data according to elevation, which may introduce uncertainty. TEM is run on monthly time scale. We averaged the daily climate data to monthly before resampling.

3. Results

3.1 Model validation

We validated TEM with monthly observation data of DST and NEP for three dominant ecosystems on the QTP (Figure 1). TEM well reproduced the seasonal variation of DST and NEP at all the three sites, with R^2 greater than 0.9 and 0.8 for DST and NEP, respectively. Simulated SOC and SON at these three sites are closed to observations (Table S1).

Apart from these three sites, we also compared the simulated SOC and SON with 289 observations on the Plateau (Figure 2 and Figure S2). The discrepancies between modeled and observed data (Figure S2) for SOC and SON may be due to the following reasons. First, the calculated SOC and SON in this study are C and N stocks in active layers, while the observations represent C and N stocks in top two meters (top three meters for 173 sites for SON; Kou et al., 2019) of soil profile. The mean ALT on the QTP is estimated at about 2.3 m during 2006–2015. By comparison, ALT is shallower than 2 m in the northwestern, eastern, and southern QTP (Ni et al., 2021; Wang, T. et al., 2020). According to Ding et al. (2016), Kou et al. (2019), and Wang et al. (2020), about half of the observation sites are distributed in the regions where ALT is estimated less than 2 m. As a result, the simulated SOC and SON in active layer is smaller than observations (Figure 2). Second, although the heterogeneities in topography, vegetation, and soils were considered by running the model on 0.1 × 0.1 degree of spatial resolution, the great spatial heterogeneities in SOC (Mishra et al., 2021) and SON make it difficult to predict site level observations based on large grid simulations.

In general, the simulated SOC and SON are comparable to observations based on the means across vegetation types (Figure 2). For the entire permafrost regions on the QTP, the estimated SOC stocks in the QTP active layers during 2006–2015 under the RCP 4.5 scenario is 15.64±0.78 Pg C (mean ± SD), a little higher than 13.22 Pg C estimated by Wang, T. et al. (2020), but lower than 19.0±6.6 Pg C (in 0–2 m soils) estimated by Mu et al. (2020). The simulated ALT during 2006–2015 (2.72±0.07 m) is close to but a little higher than 2.34±0.70 m estimated by Wang, T. et al. (2020). The climate forcing data of RCP 4.5 scenario other than meteorological observations might cause this difference. SON stocks in alpine grassland active layers during 2013–2014 are estimated at 1.47±0.04 kg N/m^2, which is within the range (1.40–1.76 kg N/m^2) estimated based on observation data within 0–3 m soil depth (Kou et al., 2019). Estimated NPP in the whole QTP is 240.99±14.27 g C $/m^2/yr$, which is close to the upper bound of the MODIS normalized difference vegetation index (NDVI) based estimate of 219.8–242.5 g C $/m^2/yr$ during 2002–2012 (Wang, S. et al., 2017). The use of RCP 4.5 data and the different time spans may be responsible for the higher estimate in this study.

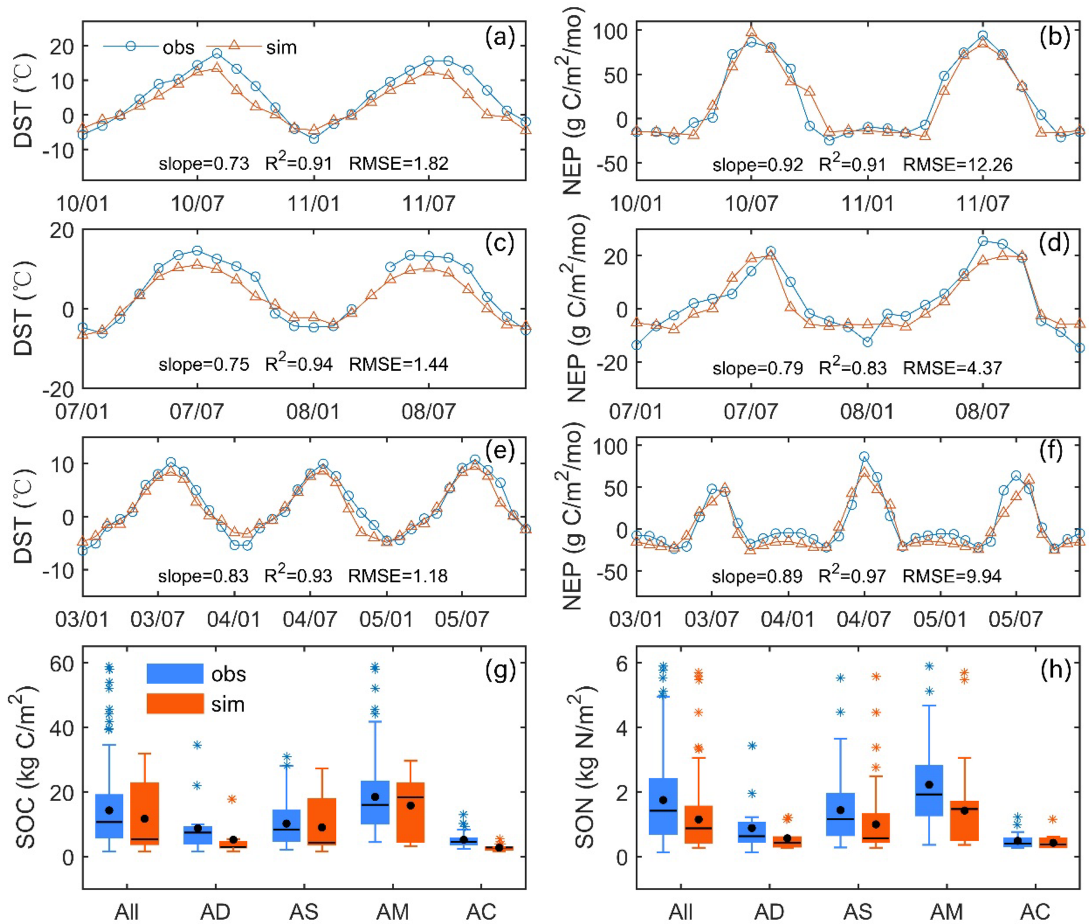

Figure 2. Comparison of model simulation (sim) with observations (obs) for soil temperature (DST) and NEP at alpine meadow (**a** and **b**), alpine steppe (**c** and **d**), and alpine shrub (**e** and **f**) sites, respectively. See Table S1 for detailed information of the observation sites. **g** and **h** represent the comparison of the simulated SOC and SON with 289 observations on the Plateau. AD, AS, AM, and AC in **g** and **h** denote alpine desert, alpine steppe, alpine meadow, and alpine cushion, respectively. The number of observation sites for AD, AS, AM, and AC are 16, 134, 106, and 33, respectively.

3.2 Changes in ecosystem C balance and the effects of ALT deepening

Permafrost regions on the QTP are projected to be a stronger C sink during the remaining of this century. VegC and SOC both increase under the RCP 4.5 and RCP 8.5 (Figure 3, S_T). As a result, by the end of this century, ecosystem C stocks (total VegC and SOC) would increase by 2.68±0.22 Pg C (0.17±0.02 Pg C gains from VegC and 2.51±0.26 Pg C gains from SOC) and 5.61±0.36 Pg C (0.44±0.08 Pg C gains from VegC and 5.18±0.35 Pg C gains from SOC), respectively, under the RCP 4.5 and RCP 8.5 scenarios. Under the RCP 4.5, the increases in NPP and RH are close, which are 53.99±24.58 Tg C/yr and 48.96±4.19 Tg C/yr, respectively. However, under the RCP 8.5, the increase in NPP (157.93±21.08 Tg C/yr) is much higher than RH (104.37±22.30 Tg C/yr). The permafrost regions on the QTP would sequestrate more C under the RCP 8.5.

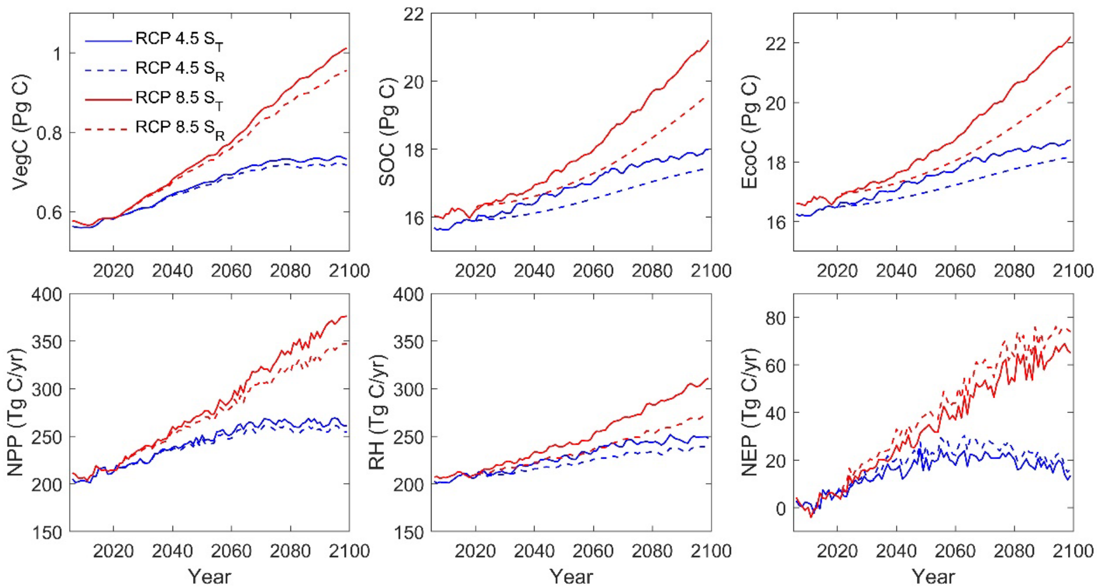

Figure 3. Changes in C pools (VegC, SOC, and EcoC) and fluxes (NPP, RH, and NEP) of the permafrost regions on the QTP in the 21st century. Differences between the results of the transient simulation (S_T) and referenced simulation (S_R) represent the direct effects of ALT. Standard deviation for each simulation did not show for clarity.

The effects of ALT deepening on C balance are represented by the difference between S_T and S_R. Figure 3 shows that ALT deepening have evident effects on C balance. We calculated the contribution of ALT deepening effects to C balance change by dividing the difference in S_T and S_R from the overall C balance changes (Figure 4b). Under the RCP 4.5, ALT deepening can contribute 9–18% of the C balance changes, and the contributions increase to 12%–37% under the RCP 8.5. The radical change in ALT (Figure 4a) under the RCP 8.5 results in a greater contribution. Under both RCPs, the deepening of ALT has more influences on SOC and RH than VegC and NPP (Figure 3 and Figure 4b).

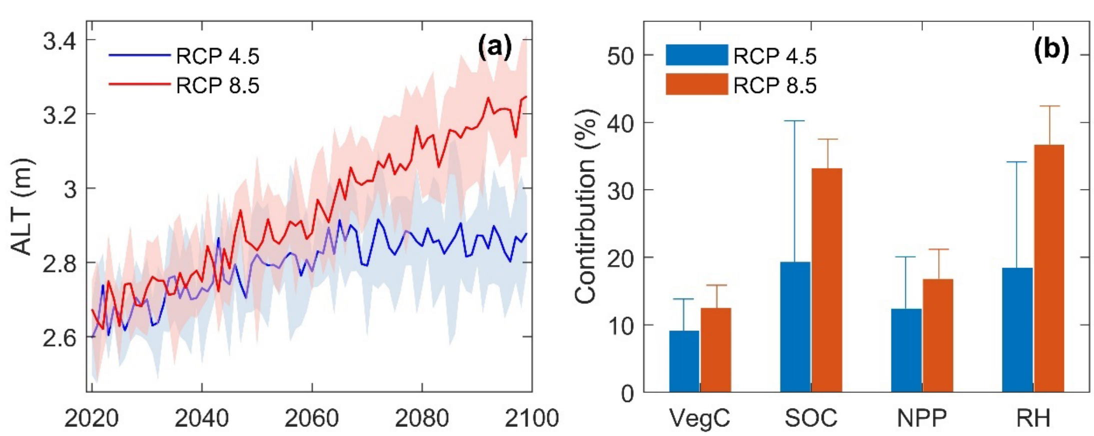

Figure 4. (a) Changes in mean ALT of the QTP under the RCP 4.5 and RCP 8.5 scenarios; **(b)** Contributions of ALT deepening effects to the overall C balance changes caused by climate change in permafrost regions of QTP during the 21st century. The shade in **(a)** and error bars in **(b)** denotes the standard deviation among all GCMs.

The greater values of S_T than S_R (Figure 3) under both RCPs suggest that ALT deepening increases ecosystem C storage in the region. However, it should be noted that the increasing in RH (9.54±5.20 (RCP 4.5) and 38.72±17.49 (RCP 8.5) Tg C/yr) is greater than NPP (6.95±5.28 (RCP 4.5) and 27.97±12.82 (RCP 8.5) Tg C/yr) due to ALT deepening (Figure 3 and Figure S3), resulting in a smaller NEP in S_T than S_R. This result illustrates that, although NPP increases more than RH in the S_T simulation (Figure 3), resulting in a stronger C sequestration over time, permafrost degradation itself strengthens RH more than NPP and cumulatively decrease NEP by 303.55±254.80 (RCP 4.5) and 518.43±234.04 (RCP 8.5) Tg C during 2020–2099.

3.3 Responses of C balance to ALT deepening in different ecosystems

The effects of ALT deepening on C balance of the QTP show an obvious spatial heterogeneity (Figure 5). The east and south parts of the QTP would increase more in both C pools and fluxes than the northwestern part due to ALT deepening, and the spatial heterogeneity is more noticeable under the RCP 8.5 than RCP 4.5. Given that east and south parts of the QTP are dominated by alpine meadow ecosystems and the northwestern part is dominated by alpine steppe ecosystems (Figure 1), these results suggest that ALT deepening has greater influence on C balance of alpine meadow than alpine steppe, particularly under the RCP 8.5. Moreover, changes in regional average ALT of these two ecosystems (Figure 6) show that increase in ALT is smaller in alpine meadow. However, C storage and fluxes of alpine meadow respond more significantly to ALT deepening.

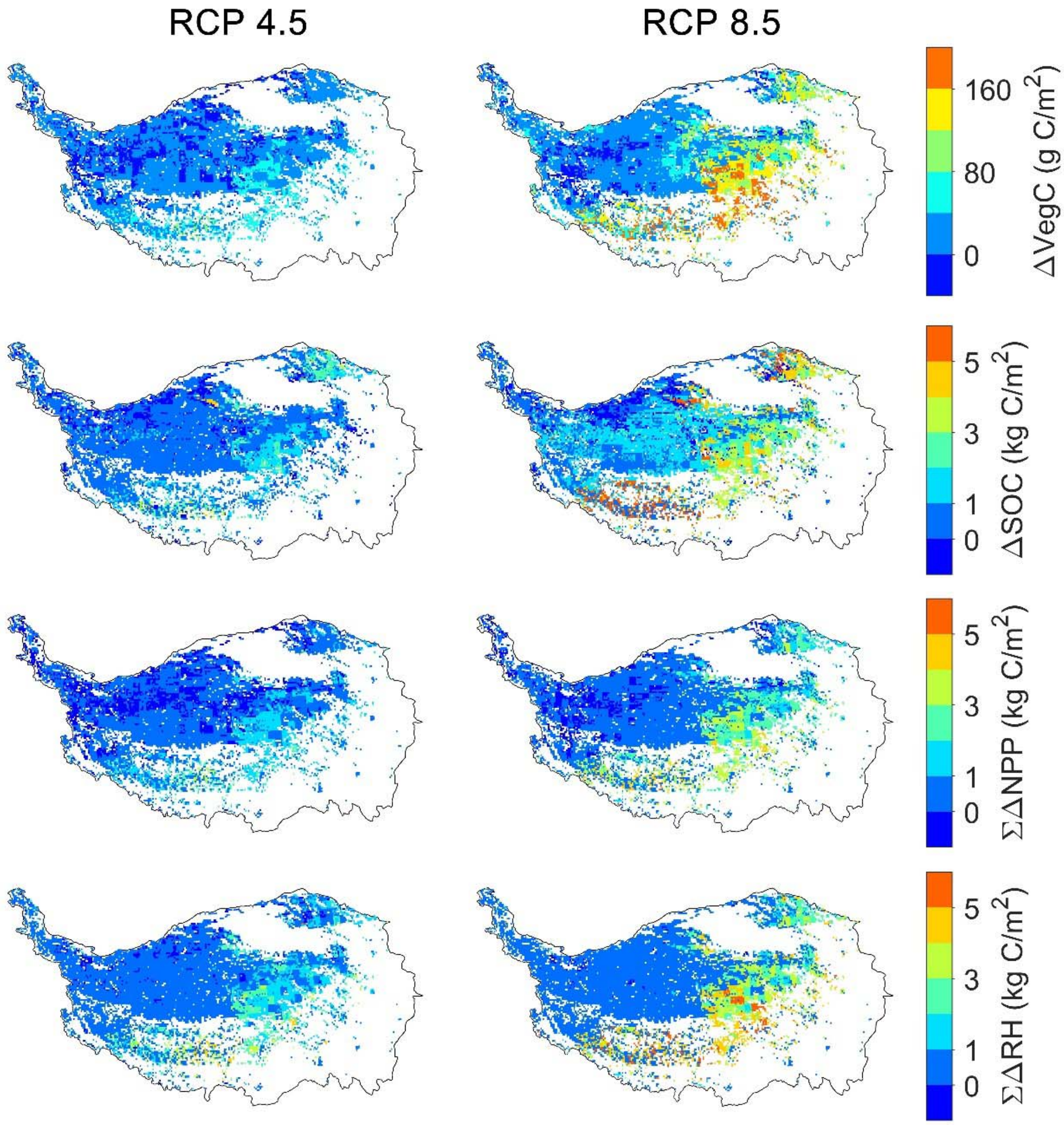

Figure 5. Changes in C balance of the QTP due to permafrost degradation under the RCP 4.5 and RCP 8.5. Δ before VegC and SOC mean the difference between the results of the transient simulation and referenced simulation (S_T-S_R) in 2099, and ∑ denotes the accumulation of each C flux from 2020 to 2099.

Under both RCPs and both ecosystems, the increasing in RH is greater than NPP (Figure 6), which is consistent with the results of the whole permafrost region (Figure 3), suggesting again that the direct effects of ALT deepening would weaken C sequestration. When comparing the two types of ecosystems, the C sequestration weakening tends to be stronger in alpine steppe ecosystems. The cumulative difference in NEP between S_T and S_R from 2020 to 2099 are -122.56±112.45 and -236.94±139.55 Tg C for alpine meadow under the RCP 4.5 and RCP 8.5, respectively, and -172.65±168.75 and -247.32±97.27 Tg C for alpine steppe under the RCP 4.5 and RCP 8.5, respectively. Given that the increasing in ALT in alpine steppe is about twice as much as that in alpine meadow (Figure 6), the C sequestration could reduce more in alpine meadow than alpine steppe with the same degree of ALT deepening.

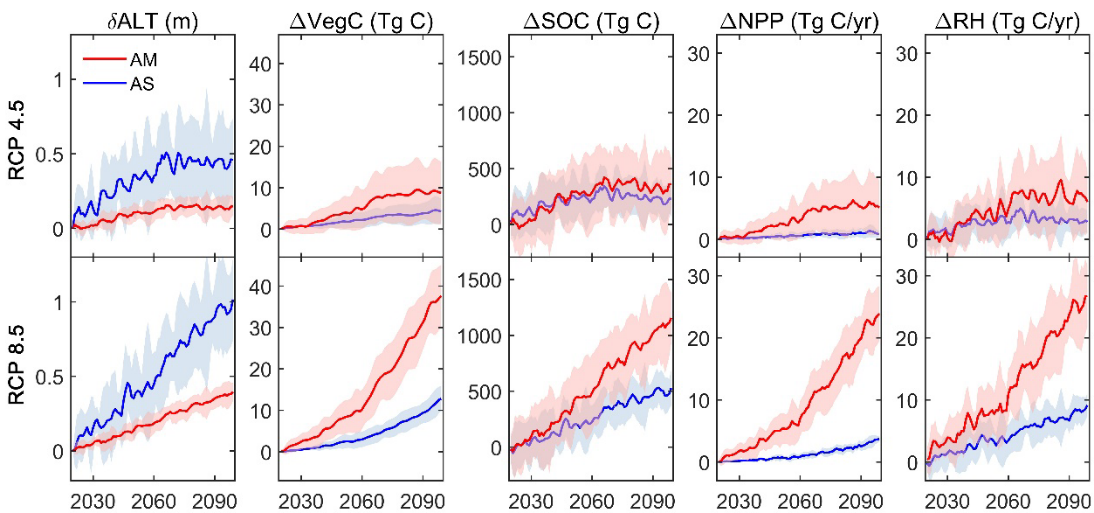

Figure 6. Anomalies of ALT from 2020 baseline and the effects of ALT deepening on ecosystem C balance of alpine meadow (AM) and alpine steppe (AS) ecosystems under the RCP 4.5 and RCP 8.5 scenarios. δ before ALT means the anomalies of ALT from 2020 baseline, and Δ before C balance components mean the difference between the results of the transient simulation and referenced simulation (S_T-S_R). Red and blue shade denotes the standard deviation among all GCMs for alpine meadow and alpine steppe ecosystems, respectively.

4. Discussion

4.1 Comparison with other studies

The estimated NPP and RH of the permafrost region on the QTP are 202.5 and 201.1 g C/m^2/yr during 2006–2011, both within the range of other estimates (120.8–329.6 g C/m^2/yr for NPP and 149.8–303.5 g C/m^2/yr for RH; Table 1). However, our NEP estimates are smaller than others. Particularly, our estimates with this version of TEM tends to be in low end of other TEM estimates, which is most likely due to more respiration from deep active layer in this study. In addition, this study focused on the permafrost region on the QTP, while Zhuang et al. (2010) and Jin et al. (2015) studied the entire QTP, and Yan et al. (2015) focused on grasslands on the QTP. Different study areas and ecosystem types considered in these studies may contribute to the discrepancies.

Existing studies show large differences in future carbon dynamics in the region (Table 1). Our estimation of flux density is higher than Jin et al. (2015) but smaller than Bosch et al. (2017). RH estimation of Bosch et al. (2017) depends only on annual precipitation, which may induce large uncertainties in their future projection because important factors like soil temperature and SOC quality and quantity were not considered. Thawing-induced CO_2 emissions are also considered in the study of Bosch et al. (2017). However, the potential C loss from thawing permafrost is estimated from incubation experiments with soil samples from the arctic region. SOC density on the QTP (14.4–17.5 kg/m^2 for alpine meadow and 6.6–7.7 kg/m^2 for alpine steppe in 0–2 m; Mu et al., 2020) can be substantially lower than that in the arctic (55.1±18.9 kg/m^2 for lowlands and 40.6±22.7 kg/m^2 for uplands in upper 1 m layer of the North American Arctic; Ping et al., 2008), which may cause an overestimate of RH in Bosch et al. (2017). The projections of Jin et al (2015) are lower for NPP and NEP in the 2090s under the RCP 8.5. TEM used in Jin et al (2015) was mainly calibrated for wetland ecosystems. Under the high warming scenario of the RCP 8.5, warming induced high evapotranspiration may result in water stress and suppress NPP for wetland ecosystems. In this study, TEM has been calibrated with the main ecosystems on the QTP, including alpine meadow, alpine steppe, alpine shrubland, and alpine desert. Different calibrations should partially contribute to the differences in those projections.

Table 1. Estimated regional C fluxes on the QTP from different studies. Units for regional total C fluxes are Tg C/yr, and units for regional mean flux density are g C/m^2/yr.

Model	Area (10^6 km^2)	Period	NPP		RH		NEP		Source
			Total	Density	Total	Density	Total	Density	
CENTURY	1.41	1901–2010	344.0	244.7	336.5	239.0	7.5	5.3	Lin et al. (2017)
TEM	1.01	1961–2010	193.0	193.7	182.9	183.7	10.1	10.0	Yan et al. (2015)
ORCHIDEE	1.39	1961–2009	219.8	158.1	208.2	149.8	11.6	8.3	Piao et al. (2012)
CASA	1.47	1982–2009	177.2	120.8					Zhang et al. (2014)
ORCHIDEE	1.39	1980–2010	323.9	233.0					Tan et al. (2010)
DOS-TEM		1981–2012		199.0		195.0		4.0	Yi et al. (2014)
TEM	1.37	1990s	451.6	329.6	415.8	303.5	35.8	26.1	Zhuang et al. (2010)
TEM	1.38	2006–2011	235.8	170.9	221.5	160.5	14.4	10.4	Jin et al. (2015)
		2090s[2]	319.9	231.8	247.1	198.7	45.8	33.1	
		2090s[3]	348.4	252.5	321.5	233.0	27.0	19.5	
RG[1]		2050[2]				388.6			Bosch et al. (2017)
		2050[3]				391.2			
		2070[2]				385.9			
		2070[3]				389.2			
TEM (S_T)	1.19	2006–2011[2]	242.1	202.5	240.5	201.1	1.6	1.3	This study
		2090s[2]	315.1	263.6	296.2	247.8	18.9	15.8	
		2090s[3]	441.2	369.0	363.2	303.8	78.0	65.2	

Notes: 1. RG denotes regression model; 2 and 3 represent estimations derived from the RCP 4.5 and RCP 8.5, respectively.

4.2 Impact of climate change on ecosystem C balance

Although permafrost degradation contributes a fraction to the overall changes in C balance (Figure 4), the differences between S_T and S_R shows that climate change is still a main factor affecting various ecosystem C processes, controlling the carbon balance (Figure 3). By

2099, ecosystem C storage and NEP of the permafrost region on the QTP would increase by 1.67±0.32 Pg C and 15.64±3.52 Tg C/yr under the RCP 4.5 and 3.65±0.49 Pg C and 70.56±9.43 Tg C/yr under the RCP 8.5, respectively. Six earth system models from phase five of the Coupled Model Inter-comparison Project (CMIP5) that did not consider the effects of permafrost degradation on SOC stocks show that NPP and RH increase from 1850 to 2100, and the carbon sink of the QTP would be higher during 2006–2100 in comparison with 1850–2005 under RCP4.5 scenario (Li et al., 2015). Increasing net nitrogen mineralization rate enhanced N availability, together with warming air temperature and rising CO_2 concentrations, promote the regional C sink on the QTP (Zhuang et al., 2010).

In the northern high latitudes, warming and elevated atmospheric CO_2 concentration have been found as key drivers to NPP and RH dynamics, but precipitation changes are less important (McGuire et al., 2018). In contrast, on the QTP, air temperature, precipitation, and atmospheric CO_2 concentration in permafrost regions would all increase under both the RCPs (Figure S4). Evidence from experimental warming (Ganjurjav et al., 2016; Zhao, J. et al., 2019), model simulation (Zheng et al., 2020), and meta-analysis (Wang, G. et al., 2019) all suggest that C exchange in alpine meadow is mainly regulated by air temperature, but C exchange in dry alpine steppe is dominated by water conditions. Given that the cover of alpine steppe (7.5×10^5 km^2) is approximately three times higher than alpine meadow (2.5×10^5 km^2) (Ni, 2000), increment in precipitation should also be associated with C exchanges in the permafrost regions on the QTP as warming and elevated atmospheric CO_2 concentration (Chen, B. et al., 2014; Piao et al., 2012;) do. Carbon dynamics responses on the QTP can be different from the conclusion of McGuire et al. (2018) for northern permafrost regions.

4.3 Nitrogen subsidies from permafrost degradation

Permafrost degradation will not only release old carbon but also supply additional nitrogen that can be utilized to boost plant productivity. The direct effects of permafrost thaw would increase ecosystem C storage and enhance C cycling on the QTP in the remaining of this century (Fig 2 and 4). Our analysis suggests that N subsidies from permafrost degradation should be the main reason for these increases in C storages and fluxes. When considering N addition, soil organic N (SON) experiences a remarkable surge in S_T (73.58±37.79 (RCP 4.5) and 156.92±21.48 (RCP 8.5) Tg N) and changes from decrease in S_R (-2.13±1.63 (RCP 4.5) and -4.12±1.80 (RCP 8.5) Tg N) to a large amount of increase in S_T (Figure 7). The increase of N availability enhances plant N uptake (VegNup; S_T-S_R: 12.41±4.72 (RCP 4.5) and 26.56±13.03 (RCP 8.5) Tg N/yr) and makes plant gain more N (VegN; S_T-S_R: 0.62±0.46 (RCP 4.5) and 1.97±0.90 (RCP 8.5) Tg N), which therefore, stimulate plant growth and increase NPP.

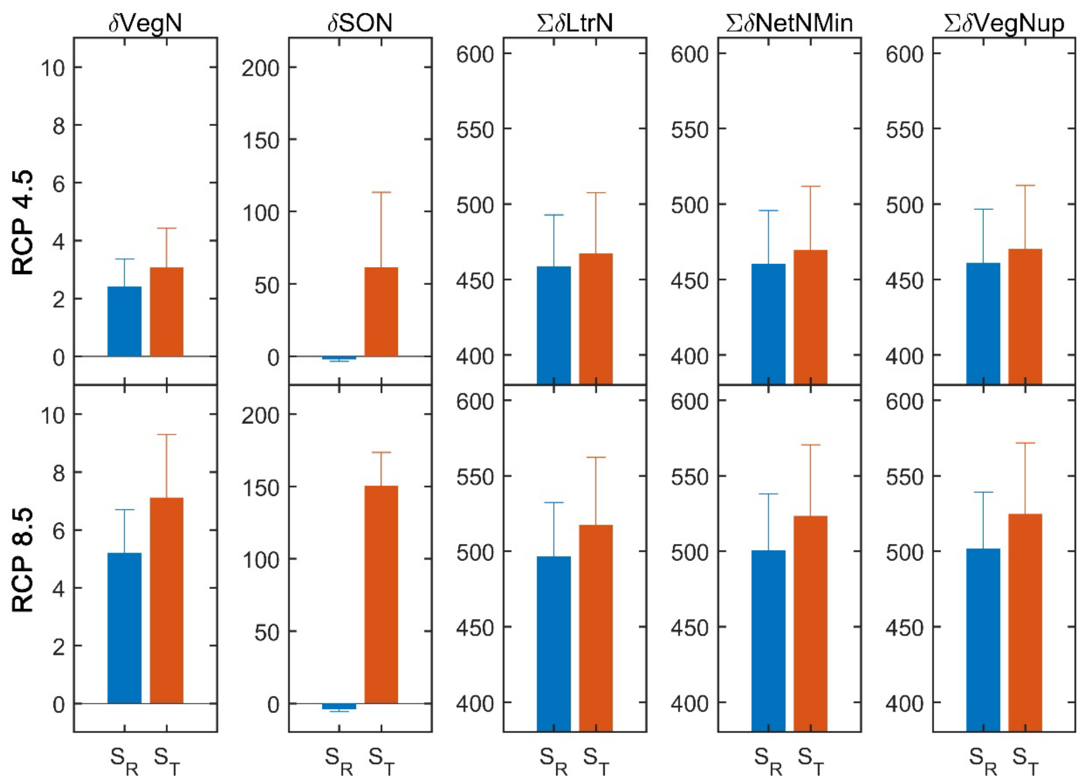

Figure 7. Changes in ecosystem N balance from 2020 baseline for the referenced simulation (S_R) and transient simulation (S_T) under the RCP 4.5 and RCP 8.5 scenarios. δ means the anomalies of N pools of 2099 from 2020 baseline; ∑ denotes the accumulation of each N flux from 2020 to 2099. The error bars represent the standard deviation among all GCMs. Units for N pools (vegetation N (VegN) and soil organic N (SON)) are Tg N, and units for N fluxes (litter N (LtrN), net N mineralization (NetNMin), and vegetation N uptake (VegNup)) are Tg N/yr.

However, although both VegN and SON benefit from permafrost thaw, the increase in VegN is much smaller than in SON (Figure 7). Based on soil C and N balance, this study estimated that 0.98±0.49 and 2.17±0.38 Pg C of SOC, and 76.14±39.45 and 162.90±23.44 Tg N of SON will be added to active layer due to permafrost thaw (Table 2), under the RCP 4.5 and RCP 8.5, respectively. Among them, 57–63% of these additional C would be consumed by microbes and discharged through RH. However, only 10–13% of these addition N would be absorbed by plant.

Figure S5 shows that N subsidies from permafrost thaw only alleviates plant N limit slightly. We find that although there is a large amount of N added to active layer due to permafrost thaw, only a small fraction of the amount can be accessed by plant. The average maximum rooting depth in permafrost regions on the QTP is estimated as 1.2 m, while the average ALT would increase to 2.9±0.1 and 3.3±0.1 m under the RCP 4.5 and RCP 8.5, respectively (Figure 4a), which is much greater than rooting zone depth. Therefore, only a small fraction of N released from thawed permafrost is absorbed by plant. The benefit of permafrost thaw is limited, but the consequence of permafrost thaw to C emission is large. As a result, the net effect of permafrost thaw on the QTP is to weaken C sequestration. Similar results have also been found over the circumpolar permafrost regions. Permafrost thaw from 1970 to 2006 exposed 11.6 Pg C of SOC to decomposition, resulting in 4.03 Pg C emission but only 0.3 Pg C compensated by the stimulated plant C uptake (Hayes et al., 2014). In the forests of Northern Eurasia, the gain of vegetation C that is benefited from N supply due to permafrost degradation is only 29.8% (RCP4.5) to 49.2% (RCP8.5) of the loss of soil organic C. Permafrost degradation overall diminishes C sequestration in these forests (Kicklighter et al., 2019). Although N released from new thawed permafrost can be used to stimulate plant productivity, plant may not be N limited or may not access to them (Koven, Lawrence et al., 2015). However, new released SOC will be decomposed, although part of them take a longer time. Consequently, the stimulated RH may overwhelm the NPP increase (due to more available N to plant from thawing permafrost), decreasing the regional C sequestration.

Table 2. Changes in soil C and N balance due to permafrost thaw.

C	ΔSOC	∑ΔLtrC	∑ΔRH	SOC_{PF}	∑ΔRH/ SOC_{PF}
RCP 4.5	0.65±0.26	0.33±0.27	0.66±0.53	0.98±0.49	0.57±0.41
RCP 8.5	1.59±0.21	0.84±0.49	1.42±0.74	2.17±0.38	0.63±0.24
N	ΔSON	∑ΔLtrN	∑ΔNetNMin	SON_{PF}	∑ΔVegNup/ SON_{PF}
RCP 4.5	75.57±39.08	8.46±7.18	9.04±7.69	76.14±39.45	0.10±0.09
RCP 8.5	160.93±22.55	20.84±12.12	22.81±13.05	162.90±23.44	0.13±0.06

Notes: Δ means the differences between the transient simulation and referenced simulation (S_T-S_R); ∑Δ means the cumulative of S_T-S_R from 2020 to 2099; SOC_{PF} and SON_{PF} mean SOC, and SON added to active layers from permafrost thaw, respectively. LtrC, LtrN, NetNMin, and VegNup denote litter C, litter N, net N mineralization, and vegetation N uptake, respectively. Units for C and N variables are Pg C and Tg N, respectively.

There are several reasons in the limited plant access to N released from permafrost degradation on the QTP. First, ALT (greater than 2 m; Ni et al., 2021; Wang, T. et al., 2020; Wu, X.B. et al., 2018) on the QTP is already much deeper than rooting depth (generally smaller than 30 cm; Yang et al., 2009) currently. N released from further deep permafrost in the future, therefore, could be far beyond plant accessibility if there are no substantial changes in plant species. Second, N mineralization in permafrost soils on the QTP has been found largely regulated by microbial traits (Mao et al., 2020; Zhang et al., 2020). Microbial biomass in permafrost on the QTP is 91.3% lower than that in active layer soils (Mao et al., 2020). The low abundance of microbes can become a key restriction on N mineralization after permafrost thaw, because of the direct role that microbes play in N transformation (Schimel and Bennett, 2004) and the positive effects of the extracellular enzymes (Ali et al., 2021; Luo et al., 2017) and microbial biomass (Li, Z. et al., 2019; Wu, H. et al., 2021) on soil N mineralization. Apart from microbial biomass, the higher abundance of bacteria than fungi in QTP permafrost may also has negative impacts on net N mineralization processes (Mao et al., 2020), because of the significantly higher metabolic N-demand and immobilization in bacteria than fungi (Kooijman et al., 2016). Further, the phase lag of heat transfer into deep soils can shift the deep soil organic matter mineralization later into fall and winter, producing a seasonal offset from the peak period of N demand during spring and summer (Koven, Lawrence et al., 2015), and reducing the access of plant to the additional N released from deep permafrost thaw. The remaining large fraction of N that cannot be used by plant could leach into aquatic ecosystems, causing far-reaching consequences on their functions and structure (Guo et al., 2019; Wickland et al., 2018), or could be lost via gaseous form of N_2O through nitrification and denitrification processes (Elberling et al., 2010; Voigt et al., 2017, 2020; Wilkerson et al., 2019), intensifying non-carbon feedback to climate warming (IPCC, 2013; Xu et al., 2012; Yang, G. et al., 2018). Considering the serious consequences and the large amount of these additional N, sufficient attention should be paid to their fate on the QTP.

4.4 Nitrogen subsidy regimes from ALT deepening in different ecosystems

The more pronounced influences of ALT deepening on C balance in alpine meadow than alpine steppe on the QTP can be due to different C and N subsidies from permafrost thaw. Although the increase in ALT is smaller in alpine meadow comparing to alpine steppe, alpine meadow gains more C and N (Figure 6 and Figure 8). The maximum rooting depth of alpine meadow and alpine steppe ranges from 0.5 to 1.9 m, but the average ALT in alpine meadow (2.05±0.01 m) is shallower than alpine steppe (2.96±0.03 m) currently. Although ALT increases more in alpine steppe, it mainly occurs in deep soils far from rooting zone, therefore, only very limited N released from thawed permafrost can be accessed by alpine steppe. On the contrary, owing to the shallower ALT in alpine meadow, more N released from thawed permafrost is within its rooting zone, thus can be used. The addition of SOC and SON released from permafrost degradation in these two ecosystems (Table 3) support such explanations.

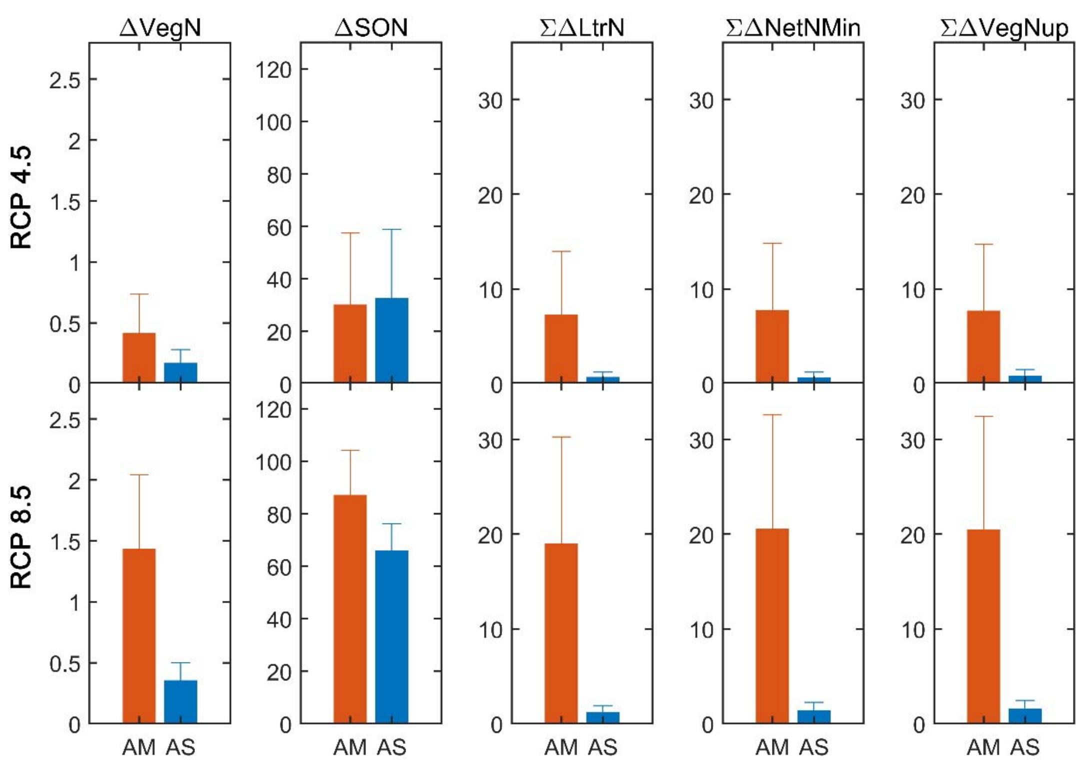

Figure 8. Differences in N balance between alpine meadow (AM) and alpine steppe (AS) ecosystems due to ALT deepening. Δ means the simulation differences between the transient

simulation and referenced simulation (S_T-S_R) in 2099; ∑ denotes the accumulative differences in N fluxes from 2020 to 2099. The error bars represent standard deviations among all GCMs. Units for N pools (vegetation N (VegN) and soil organic N (SON)) are Tg N, and units for N fluxes (litter N (LtrN), net N mineralization (NetNMin), and vegetation N uptake (VegNup)) are Tg N/yr.

In addition, SOC and total nitrogen stocks in alpine meadow is about twice of that in alpine steppe on the QTP (Ding et al., 2016; Zhao, L. et al., 2018), which may result in the significant increasing in ecosystem C and N pools in alpine meadow ecosystem even with less increases in ALT. The higher density of SOC underneath alpine meadow can provide more substrates for microbe than that underneath alpine steppe, triggering a stronger RH response (Crowther et al., 2016). More SOC can also stimulate microbial activities and increase microbial biomass in alpine ecosystems (Li, Y. et al., 2019), strengthening RH. Apart from quantity, incubation experiments found that SOM under alpine meadow is highly decomposable (Chen, L. et al., 2016), while SOM under steppe is largely composed of stable organic compounds (Wu, X. et al., 2014). These differences may also contribute to a more sensitive RH in alpine meadow ecosystems (Eberwein et al., 2015). The consumption of SOC that released from permafrost thaw (Table 3) also shows that most of the additional SOC (79–85%) in alpine meadow would be consumed by microbe through RH, while only nearly a half (44–51%) of them would be consumed in alpine steppe.

The stronger response of ΔNPP to ALT in alpine meadow can partly be explained by the significantly higher usage of N supplied by permafrost thaw (Table 3). More than 25% of additional N is utilized in alpine meadow, while only less than 3% is absorbed by alpine steppe, therefore, contributing to distinct vegetation responses in ΔNPP. Alpine meadow ecosystem is mainly distributed in the eastern QTP. Relatively adequate precipitation, but also cold climate makes alpine meadow has higher soil water content than alpine steppe, which is distributed in arid climate. High soil water content in alpine meadow can facilitate N utilize by plant as water availability influences the diffusion of soil N to plant (Humbert et al., 2016; Simkin et al., 2016). Conversely, water limiting in alpine steppe constrains its nutrient availability and make it respond differently to climate warming and nitrogen addition from alpine meadow (Ganjurjav et al., 2016; Li, S. et al., 2019; Zheng et al., 2020). Different water conditions in these two ecosystems may result in distinct differences in N usage (Table 3) and fluxes (Figure 8).

Table 3. Changes in SOC and SON in alpine meadow and alpine steppe ecosystems due to permafrost thaw.

	Alpine meadow		Alpine steppe	
C	SOC_{PF}	$\sum\Delta RH/ SOC_{PF}$	SOC_{PF}	$\sum\Delta RH/ SOC_{PF}$
RCP 4.5	0.57±0.31	0.85±0.22	0.42±0.25	0.51±0.29
RCP 8.5	1.40±0.37	0.79±0.30	0.79±0.14	0.44±0.13
N	SON_{PF}	$\sum\Delta VegNup/ SON_{PF}$	SON_{PF}	$\sum\Delta VegNup/ SON_{PF}$
RCP 4.5	30.70±29.23	0.31±0.13	32.60±27.48	0.02±0.00

RCP 8.5	88.73±18.62	0.25±0.09		66.15±7.41	0.03±0.01

Notes: $\sum\Delta$ means the cumulative difference between the transient simulation and referenced simulation (S_T-S_R) from 2020 to 2099; SOC_{PF} and SON_{PF} mean SOC, and SON added to active layers from permafrost thaw, respectively. Units for soil C and N are Pg C and Tg N, respectively.

5. Conclusions

We modified a process-based biogeochemistry model by considering the effects of extra carbon and nitrogen from thawing permafrost to quantify ecosystem C balance on the Qinghai-Tibetan plateau in the 21st century. Permafrost regions on the plateau would sequestrate more C and become a stronger C sink by the end of this century under both RCP 4.5 and RCP 8.5 scenarios. However, permafrost degradation on the QTP is projected to diminish the ecosystem C sequestration capacity, because the increase of NPP stimulated by N supply from thawing permafrost is smaller than the enhanced soil carbon respiration. Due to the deep active layer on the QTP, N released from thawing permafrost is mainly distributed in deep soils, which is not accessible by plant, thus having a limited benefit to plant carbon uptake. As a result, the C sink would decrease by 303.55±254.80 (RCP 4.5) and 518.43±234.04 (RCP 8.5) Tg C during 2020–2099.

Permafrost degradation on the QTP has different effects on C balance of the distinct ecosystems of alpine meadow and alpine steppe. C storages and fluxes respond more significant to ALT deepening in alpine meadow than alpine steppe, which could be due to the shallower ALT, the higher C and N stocks, and the wetter environment in alpine meadow.

Although more than half of the C released from thawing permafrost would be decomposed and emitted into the atmosphere, only 10% of the released N is utilized by plant. The remaining large amount of N could have significant impacts on aquatic ecosystems and may intensify climate warming through another potent greenhouse gas N_2O release. Therefore, the study on this gas release shall draw sufficient attention on the plateau.

This study highlights the important effects of permafrost thaw on C and N cycling in permafrost dominated ecosystems and underscore the critical role of factoring deep permafrost carbon into land surface modeling in order to make more reliable projections of future permafrost carbon-climate feedbacks.

Acknowledgements

This study is funded by the Second Tibetan Plateau Scientific Expedition and Research Program (SQ2019QZKK2003), National Natural Science Foundation of China (41571193), and the ‘Strategic Priority Research Program’ of the Chinese Academy of Sciences (XDA20020202). We gratefully acknowledge financial support from China Scholarship Council. We also thank the ISIMIP cross sectoral science team for their roles in producing, coordinating, and making available the ISIMIP2b data (available at https://esg.pik-potsdam.de/search/isimip/). The authors declare no conflict of interest.

References

Abbott, B. W., Jones, J. B., Schuur, E. A. G., Chapin Iii, F. S., Bowden, W. B., Bret-Harte, M. S., et al. (2016), Biomass offsets little or none of permafrost carbon release from soils, streams, and wildfire: An expert assessment. *Environmental Research Letters*, *11*(3), 034014. doi: 10.1088/1748-9326/11/3/034014

Ali, S., Dongchu, L., Jing, H., Ahmed, W., Abbas, M., Qaswar, M., et al. (2021), Soil microbial biomass and extracellular enzymes regulate nitrogen mineralization in a wheat-maize cropping system after three decades of fertilization in a chinese ferrosol. *Journal of Soils and Sediments*, *21*(1), 281-294. doi: 10.1007/s11368-020-02770-5

Bosch, A., Schmidt, K., He, J.-S., Doerfer, C., & Scholten, T. (2017), Potential co2 emissions from defrosting permafrost soils of the Qinghai-Tibet plateau under different scenarios of climate change in 2050 and 2070. *CATENA*, *149*, 221-231. doi: https://doi.org/10.1016/j.catena.2016.08.035

Burke, E. J., Ekici, A., Huang, Y., Chadburn, S. E., Huntingford, C., Ciais, P., et al. (2017), Quantifying uncertainties of permafrost carbon-climate feedbacks. *Biogeosciences*, *14*(12), 3051-3066. doi: 10.5194/bg-14-3051-2017

Burke, E. J., Jones, C. D., & Koven, C. D. (2013), Estimating the permafrost-carbon climate response in the cmip5 climate models using a simplified approach. *Journal of Climate*, *26*(14), 4897-4909. doi: 10.1175/JCLI-D-12-00550.1

Chen, B., Zhang, X., Tao, J., Wu, J., Wang, J., Shi, P., et al. (2014), The impact of climate change and anthropogenic activities on alpine grassland over the Qinghai-Tibet plateau. *Agricultural and Forest Meteorology*, *189-190*, 11-18. doi: https://doi.org/10.1016/j.agrformet.2014.01.002

Chen, L., Liang, J., Qin, S., Liu, L., Fang, K., Xu, Y., et al. (2016), Determinants of carbon release from the active layer and permafrost deposits on the Tibetan plateau. *Nature Communications*, *7*(1), 13046. doi: 10.1038/ncomms13046

Chinese Academy of Sciences. (2001). *Vegetation Atlas of China*. Science Press, Beijing.

Crowther, T. W., Todd-Brown, K. E. O., Rowe, C. W., Wieder, W. R., Carey, J. C., Machmuller, M. B., et al. (2016), Quantifying global soil carbon losses in response to warming. *Nature*, *540*(7631), 104-108. doi: 10.1038/nature20150

Ding, J., Chen, L., Ji, C., Hugelius, G., Li, Y., Liu, L., et al. (2017), Decadal soil carbon accumulation across Tibetan permafrost regions. *Nature Geoscience*, *10*(6), 420-424. doi: 10.1038/ngeo2945

Ding, J., Li, F., Yang, G., Chen, L., Zhang, B., Liu, L., et al. (2016), The permafrost carbon inventory on the Tibetan plateau: A new evaluation using deep sediment cores. *Global Change Biology*, *22*(8), 2688-2701. doi:10.1111/gcb.13257

Eberwein, J. R., Oikawa, P. Y., Allsman, L. A., & Jenerette, G. D. (2015), Carbon availability regulates soil respiration response to nitrogen and temperature. *Soil Biology and Biochemistry*, *88*, 158-164. doi: https://doi.org/10.1016/j.soilbio.2015.05.014

Editorial Committee of Vegetation Map of China, Chinese Academy of Sciences. (2001). *Vegetation Atlas of China*. Science Press, Beijing.

Elberling, B., Christiansen, H. H., & Hansen, B. U. (2010), High nitrous oxide production from thawing permafrost. *Nature Geoscience*, *3*(5), 332-335. doi: 10.1038/ngeo803

Farr, T. G., Rosen, P. A., Caro, E., Crippen, R., Duren, R., Hensley, S., et al. (2007), The shuttle radar topography mission. *Reviews of Geophysics*, *45*(2). doi: https://doi.org/10.1029/2005RG000183

Finger, R. A., Turetsky, M. R., Kielland, K., Ruess, R. W., Mack, M. C., & Euskirchen, E. S. (2016), Effects of permafrost thaw on nitrogen availability and plant-soil interactions in a boreal Alaskan lowland. *Journal of Ecology*, *104*(6), 1542-1554. doi: 10.1111/1365-2745.12639

Frieler, K., Lange, S., Piontek, F., Reyer, C. P. O., Schewe, J., Warszawski, L., et al. (2017), Assessing the impacts of 1.5 degrees c global warming - simulation protocol of the inter-sectoral impact model intercomparison project (isimip2b). *Geoscientific Model Development*, *10*(12), 4321-4345. doi: 10.5194/gmd-10-4321-2017

Fu, Y., Liu, C., Lin, F., Hu, X., Zheng, X., Zhang, W., & Cao, G. (2018), Quantification of year-round methane and nitrous oxide fluxes in a typical alpine shrub meadow on the Qinghai-Tibetan plateau. *Agriculture, Ecosystems & Environment*, *255*, 27-36. doi: https://doi.org/10.1016/j.agee.2017.12.003

Ganjurjav, H., Gao, Q. Z., Gornish, E. S., Schwartz, M. W., Liang, Y., Cao, X. J., et al. (2016), Differential response of alpine steppe and alpine meadow to climate warming in the central Qinghai-Tibetan plateau. *Agricultural and Forest Meteorology*, *223*, 233-240. doi: 10.1016/j.agrformet.2016.03.017

Guo, Y. D., Song, C. C., Tan, W. W., Wang, X. W., & Lu, Y. Z. (2019), Export of dissolved nitrogen in catchments underlain by permafrost in northeast china. *Science of the Total Environment*, *660*, 1210-1218. doi: 10.1016/j.scitotenv.2018.12.464

Hao, A., Xue, X., Wang, X., Zhao, G., You, Q., Peng, F., et al. (2021), Different response of alpine meadow and alpine steppe to climatic and anthropogenic disturbance on the Tibetan plateau. *Global Ecology and Conservation*, *27*, e01512. doi: https://doi.org/10.1016/j.gecco.2021.e01512

Hayes, D. J., Kicklighter, D. W., McGuire, A. D., Chen, M., Zhuang, Q., Yuan, F., et al. (2014), The impacts of recent permafrost thaw on land–atmosphere greenhouse gas exchange. *Environmental Research Letters*, *9*(4), 045005. doi: 10.1088/1748-9326/9/4/045005

Hayes, D. J., McGuire, A. D., Kicklighter, D. W., Gurney, K. R., Burnside, T. J., & Melillo, J. M. (2011), Is the northern high-latitude land-based co2 sink weakening? *Global Biogeochemical Cycles*, *25*(3). doi: https://doi.org/10.1029/2010GB003813

Humbert, J. Y., Dwyer, J. M., Andrey, A., & Arlettaz, R. (2016), Impacts of nitrogen addition on plant biodiversity in mountain grasslands depend on dose, application duration and climate: A systematic review. *Global Change Biology*, *22*(1), 110-120. doi: 10.1111/gcb.12986

Huo, L., Chen, Z., Zou, Y., Lu, X., Guo, J., & Tang, X. (2013), Effect of zoige alpine wetland degradation on the density and fractions of soil organic carbon. *Ecological Engineering*, *51*, 287-295. doi: https://doi.org/10.1016/j.ecoleng.2012.12.020

IPCC, 2013: *Climate Change 2013: The Physical Science Basis*. Contribution of Working Group I to the Fifth Assessment Report of the Intergovernmental Panel on Climate Change [Stocker, T.F., D. Qin, G.-K. Plattner, M. Tignor, S.K. Allen, J. Boschung, A. Nauels, Y. Xia, V. Bex and P.M. Midgley (eds.)]. Cambridge University Press, Cambridge, United Kingdom and New York, NY, USA, 1535 pp.

Jin, Z., Zhuang, Q., He, J.-S., Luo, T., & Shi, Y. (2013), Phenology shift from 1989 to 2008 on the Tibetan plateau: An analysis with a process-based soil physical model and remote sensing data. *Climatic Change*, *119*(2), 435-449. doi: 10.1007/s10584-013-0722-7

Jin, Z., Zhuang, Q., He, J.-S., Zhu, X., & Song, W. (2015), Net exchanges of methane and carbon dioxide on the Qinghai-Tibetan plateau from 1979 to 2100. *Environmental Research Letters*, *10*(8), 085007. doi: 10.1088/1748-9326/10/8/085007

Jones, C. D., Arora, V., Friedlingstein, P., Bopp, L., Brovkin, V., Dunne, J., et al. (2016), C4MIP – the coupled climate–carbon cycle model intercomparison project: Experimental protocol for cmip6. *Geoscientific Model Development*, *9*(8), 2853-2880. doi: 10.5194/gmd-9-2853-2016

Keuper, F., van Bodegom, P. M., Dorrepaal, E., Weedon, J. T., van Hal, J., van Logtestijn, R. S. P., & Aerts, R. (2012), A frozen feast: Thawing permafrost increases plant-available nitrogen in subarctic peatlands. *Global Change Biology*, *18*(6), 1998-2007. doi: 10.1111/j.1365-2486.2012.02663.x

Kicklighter, D. W., Melillo, J. M., Monier, E., Sokolov, A. P., & Zhuang, Q. (2019), Future nitrogen availability and its effect on carbon sequestration in northern eurasia. *Nat Commun*, *10*(1), 3024. doi: 10.1038/s41467-019-10944-0

Kooijman, A. M., Bloem, J., van Dalen, B. R., & Kalbitz, K. (2016), Differences in activity and n demand between bacteria and fungi in a microcosm incubation experiment with selective inhibition. *Applied Soil Ecology*, *99*, 37-47. doi: 10.1016/j.apsoil.2015.11.011

Kou, D., Ding, J., Li, F., Wei, N., Fang, K., Yang, G., et al. (2019), Spatially-explicit estimate of soil nitrogen stock and its implication for land model across Tibetan alpine permafrost region. *Science of the Total Environment*, *650*, 1795-1804. doi: https://doi.org/10.1016/j.scitotenv.2018.09.252

Koven, C. D., Lawrence, D. M., & Riley, W. J. (2015a), Permafrost carbon-climate feedback is sensitive to deep soil carbon decomposability but not deep soil nitrogen dynamics. *Proceedings of the National Academy of Sciences of the United States of America*, *112*(12), 3752-3757. doi: 10.1073/pnas.1415123112

Koven, C. D., Ringeval, B., Friedlingstein, P., Ciais, P., Cadule, P., Khvorostyanov, D., et al. (2011), Permafrost carbon-climate feedbacks accelerate global warming. *Proceedings of the National Academy of Sciences*, *108*(36), 14769-14774. doi: 10.1073/pnas.1103910108

Koven, C. D., Schuur, E. A. G., Schadel, C., Bohn, T. J., Burke, E. J., Chen, G., et al. (2015b), A simplified, data-constrained approach to estimate the permafrost carbon-climate feedback. *Philosophical Transactions of the Royal Society a-Mathematical Physical and Engineering Sciences*, *373*(2054), 23. doi: 10.1098/rsta.2014.0423

Li, S., Dong, S., Shen, H., Han, Y., Zhang, J., Xu, Y., et al. (2019), Different responses of multifaceted plant diversities of alpine meadow and alpine steppe to nitrogen addition gradients on Qinghai-Tibetan plateau. *Science of the Total Environment*, *688*, 1405-1412. doi: https://doi.org/10.1016/j.scitotenv.2019.06.211

Li, Y., Lv, W., Jiang, L., Zhang, L., Wang, S., Wang, Q., et al. (2019), Microbial community responses reduce soil carbon loss in Tibetan alpine grasslands under short-term warming. *Global Change Biology*, *25*(10), 3438-3449. doi: https://doi.org/10.1111/gcb.14734

Li, Z. L., Tian, D. S., Wang, B. X., Wang, J. S., Wang, S., Chen, H. Y. H., et al. (2019), Microbes drive global soil nitrogen mineralization and availability. *Global Change Biology*, *25*(3), 1078-1088. doi: 10.1111/gcb.14557

Liang, J., Xia, J., Shi, Z., Jiang, L., Ma, S., Lu, X., et al. (2018), Biotic responses buffer warming-induced soil organic carbon loss in arctic tundra. *Global Change Biology*, *24*(10), 4946-4959. doi: https://doi.org/10.1111/gcb.14325

Lin, X., Han, P., Zhang, W., & Wang, G. (2017), Sensitivity of alpine grassland carbon balance to interannual variability in climate and atmospheric co2 on the Tibetan plateau during the last century. *Global and Planetary Change*, *154*, 23-32. doi: https://doi.org/10.1016/j.gloplacha.2017.05.008

Liu, Y., Geng, X., Tenzintarchen, Wei, D., Dai, D., & Xu, R. (2020), Divergence in ecosystem carbon fluxes and soil nitrogen characteristics across alpine steppe, alpine meadow and alpine swamp ecosystems in a biome transition zone. *Science of the Total Environment*, *748*, 142453. doi: https://doi.org/10.1016/j.scitotenv.2020.142453

Luo, L., Meng, H., & Gu, J. D. (2017), Microbial extracellular enzymes in biogeochemical cycling of ecosystems. *Journal of Environmental Management*, *197*, 539-549. doi: 10.1016/j.jenvman.2017.04.023

MacDougall, A. H., & Knutti, R. (2016), Projecting the release of carbon from permafrost soils using a perturbed parameter ensemble modelling approach. *Biogeosciences*, *13*(7), 2123-2136. doi: 10.5194/bg-13-2123-2016

Mao, C., Kou, D., Chen, L., Qin, S., Zhang, D., Peng, Y., & Yang, Y. (2020), Permafrost nitrogen status and its determinants on the Tibetan plateau. *Global Change Biology*, *26*(9), 5290-5302. doi: 10.1111/gcb.15205

McGuire, A. D., Koven, C., Lawrence, D. M., Clein, J. S., Xia, J. Y., Beer, C., et al. (2016), Variability in the sensitivity among model simulations of permafrost and carbon dynamics in the permafrost region between 1960 and 2009. *Global Biogeochemical Cycles*, *30*(7), 1015-1037. doi: 10.1002/2016gb005405

McGuire, A. D., Lawrence, D. M., Koven, C., Clein, J. S., Burke, E., Chen, G. S., et al. (2018), Dependence of the evolution of carbon dynamics in the northern permafrost region on the trajectory of climate change. *Proceedings of the National Academy of Sciences of the United States of America*, *115*(15), 3882-3887. doi: 10.1073/pnas.1719903115

McGuire, A. D., Melillo, J. M., Joyce, L. A., Kicklighter, D. W., Grace, A. L., Moore, B., & Vorosmarty, C. J. (1992), Interactions between carbon and nitrogen dynamics in estimating net primary productivity for potential vegetation in north america. *Global Biogeochemical Cycles*, *6*(2), 101-124. doi: 10.1029/92gb00219

Mishra, U., Hugelius, G., Shelef, E., Yang, Y., Strauss, J., Lupachev, A., et al. (2021), Spatial heterogeneity and environmental predictors of permafrost region soil organic carbon stocks. *Science Advances*, *7*(9), eaaz5236. doi: 10.1126/sciadv.aaz5236

Moss, R. H., Edmonds, J. A., Hibbard, K. A., Manning, M. R., Rose, S. K., van Vuuren, D. P., et al. (2010), The next generation of scenarios for climate change research and assessment. *Nature*, *463*(7282), 747-756. doi: 10.1038/nature08823

Mu, C., Abbott, B. W., Norris, A. J., Mu, M., Fan, C., Chen, X., et al. (2020), The status and stability of permafrost carbon on the Tibetan plateau. *Earth-Science Reviews*, *211*, 103433. doi: https://doi.org/10.1016/j.earscirev.2020.103433

Ni, J. (2000), A simulation of biomes on the Tibetan plateau and their responses to global climate change. *Mountain Research and Development*, *20*(1), 80-89. doi: 10.1659/0276-4741(2000)020[0080:Asobot]2.0.Co;2

Ni, J., Wu, T., Zhu, X., Hu, G., Zou, D., Wu, X., et al. (2021), Simulation of the present and future projection of permafrost on the Qinghai-Tibet plateau with statistical and machine learning models. *Journal of Geophysical Research: Atmospheres*, *126*(2), e2020JD033402. doi: https://doi.org/10.1029/2020JD033402

Nieberding, F., Wille, C., Fratini, G., Asmussen, M. O., Wang, Y., Ma, Y., & Sachs, T. (2020), A long-term (2005–2019) eddy covariance data set of co2 and h2o fluxes from the Tibetan alpine steppe. *Earth Syst. Sci. Data*, *12*(4), 2705-2724. doi: 10.5194/essd-12-2705-2020

Peng, F., Xue, X., Li, C., Lai, C., Sun, J., Tsubo, M., et al. (2020), Plant community of alpine steppe shows stronger association with soil properties than alpine meadow alongside degradation. *Science of the Total Environment*, *733*, 139048. doi: https://doi.org/10.1016/j.scitotenv.2020.139048

Peng, X., Zhang, T., Frauenfeld, O. W., Wang, S., Qiao, L., Du, R., & Mu, C. (2020), Northern hemisphere greening in association with warming permafrost. *Journal of Geophysical Research: Biogeosciences*, *125*(1), e2019JG005086. doi: 10.1029/2019jg005086

Piao, S., Tan, K., Nan, H., Ciais, P., Fang, J., Wang, T., et al. (2012), Impacts of climate and co2 changes on the vegetation growth and carbon balance of Qinghai–Tibetan grasslands over the past five decades. *Global and Planetary Change*, *98-99*, 73-80. doi: https://doi.org/10.1016/j.gloplacha.2012.08.009

Ping, C.-L., Michaelson, G. J., Jorgenson, M. T., Kimble, J. M., Epstein, H., Romanovsky, V. E., & Walker, D. A. (2008), High stocks of soil organic carbon in the north American arctic region. *Nature Geoscience*, *1*(9), 615-619. doi: 10.1038/ngeo284

Qian, H. F., Joseph, R., & Zeng, N. (2010), Enhanced terrestrial carbon uptake in the northern high latitudes in the 21st century from the coupled carbon cycle climate model intercomparison project model projections. *Global Change Biology*, *16*(2), 641-656. doi: 10.1111/j.1365-2486.2009.01989.x

Salmon, V. G., Schadel, C., Bracho, R., Pegoraro, E., Celis, G., Mauritz, M., et al. (2018), Adding depth to our understanding of nitrogen dynamics in permafrost soils. *Journal of Geophysical Research-Biogeosciences*, *123*(8), 2497-2512. doi: 10.1029/2018jg004518

Salmon, V. G., Soucy, P., Mauritz, M., Celis, G., Natali, S. M., Mack, M. C., & Schuur, E. A. G. (2016), Nitrogen availability increases in a tundra ecosystem during five years of experimental permafrost thaw. *Global Change Biology*, *22*(5), 1927-1941. doi: 10.1111/gcb.13204

Schaefer, K., Lantuit, H., Romanovsky, V. E., Schuur, E. A. G., & Witt, R. (2014), The impact of the permafrost carbon feedback on global climate. *Environmental Research Letters*, *9*(8), 085003. doi: 10.1088/1748-9326/9/8/085003

Schaphoff, S., Heyder, U., Ostberg, S., Gerten, D., Heinke, J., & Lucht, W. (2013), Contribution of permafrost soils to the global carbon budget. *Environmental Research Letters*, *8*(1), 014026. doi: 10.1088/1748-9326/8/1/014026

Schimel, J. P., & Bennett, J. (2004), Nitrogen mineralization: Challenges of a changing paradigm. *Ecology*, *85*(3), 591-602. doi: 10.1890/03-8002

Schuur, E. A. G., McGuire, A. D., Schadel, C., Grosse, G., Harden, J. W., Hayes, D. J., et al. (2015), Climate change and the permafrost carbon feedback. *Nature*, *520*(7546), 171-179. doi: 10.1038/nature14338

Shang, W., Wu, X. D., Zhao, L., Yue, G. Y., Zhao, Y. H., Qiao, Y. P., & Li, Y. Q. (2016), Seasonal variations in labile soil organic matter fractions in permafrost soils with different vegetation types in the central Qinghai-Tibet plateau. *Catena*, *137*, 670-678. doi: 10.1016/j.catena.2015.07.012

Shu, S., Jain, A. K., Koven, C. D., & Mishra, U. (2020), Estimation of permafrost soc stock and turnover time using a land surface model with vertical heterogeneity of permafrost soils. *Global Biogeochemical Cycles*, *34*(11), e2020GB006585. doi: https://doi.org/10.1029/2020GB006585

Simkin, S. M., Allen, E. B., Bowman, W. D., Clark, C. M., Belnap, J., Brooks, M. L., et al. (2016), Conditional vulnerability of plant diversity to atmospheric nitrogen deposition across the united states. *Proceedings of the National Academy of Sciences of the United States of America*, *113*(15), 4086-4091. doi: 10.1073/pnas.1515241113

Tan, K., Ciais, P., Piao, S., Wu, X., Tang, Y., Vuichard, N., et al. (2010), Application of the ORCHIDEE global vegetation model to evaluate biomass and soil carbon stocks of Qinghai-Tibetan grasslands. *Global Biogeochemical Cycles*, *24*(1). doi: https://doi.org/10.1029/2009GB003530

Tao, Z., Shen, C., Gao, Q., Sun, Y., Yi, W., & Li, Y. (2007), Soil organic carbon storage and soil co2 flux in the alpine meadow ecosystem. *Science in China Series D: Earth Sciences*, *50*(7), 1103-1114. doi: 10.1007/s11430-007-0055-3

Voigt, C., Marushchak, M. E., Abbott, B. W., Biasi, C., Elberling, B., Siciliano, S. D., et al. (2020), Nitrous oxide emissions from permafrost-affected soils. *Nature Reviews Earth & Environment*, *1*(8), 420-434. doi: 10.1038/s43017-020-0063-9

Voigt, C., Marushchak, M. E., Lamprecht, R. E., Jackowicz-Korczynski, M., Lindgren, A., Mastepanov, M., et al. (2017), Increased nitrous oxide emissions from arctic peatlands after permafrost thaw. *Proceedings of the National Academy of Sciences of the United States of America*, *114*(24), 6238-6243. doi: 10.1073/pnas.1702902114

Wang, G., Li, F., Peng, Y., Yu, J., Zhang, D., Yang, G., et al. (2019), Responses of soil respiration to experimental warming in an alpine steppe on the Tibetan plateau. *Environmental Research Letters*, *14*(9), 094015. doi: 10.1088/1748-9326/ab3bbc

Wang, L., Liu, H., Shao, Y., Liu, Y., & Sun, J. (2018), Water and co2 fluxes over semiarid alpine steppe and humid alpine meadow ecosystems on the Tibetan plateau. *Theoretical and Applied Climatology*, *131*(1), 547-556. doi: 10.1007/s00704-016-1997-1

Wang, S. Y., Zhang, B., Yang, Q. C., Chen, G. S., Yang, B. J., Lu, L. L., et al. (2017), Responses of net primary productivity to phenological dynamics in the Tibetan plateau, china. *Agricultural and Forest Meteorology*, *232*, 235-246. doi: 10.1016/j.agrformet.2016.08.020

Wang T. (2019). *Frozen ground map of China based on a Map of the Glaciers, Frozen Ground and Deserts in China*. National Cryosphere Desert Data Center (http://www.ncdc.ac.cn).

Wang, T., Yang, D., Yang, Y., Piao, S., Li, X., Cheng, G., & Fu, B. (2020), Permafrost thawing puts the frozen carbon at risk over the Tibetan plateau. *Science Advances*, *6*(19), eaaz3513. doi: 10.1126/sciadv.aaz3513

Wickland, K. P., Waldrop, M. P., Aiken, G. R., Koch, J. C., Jorgenson, M. T., & Striegl, R. G. (2018), Dissolved organic carbon and nitrogen release from boreal Holocene permafrost and seasonally frozen soils of Alaska. *Environmental Research Letters*, *13*(6), 065011. doi: 10.1088/1748-9326/aac4ad

Wieder, W. (2014), Regridded harmonized world soil database v1.2, edited, ORNL Distributed Active Archive Center.

Wilkerson, J., Dobosy, R., Sayres, D. S., Healy, C., Dumas, E., Baker, B., & Anderson, J. G. (2019), Permafrost nitrous oxide emissions observed on a landscape scale using the airborne eddy-covariance method. *Atmospheric Chemistry and Physics*, *19*(7), 4257-4268. doi: 10.5194/acp-19-4257-2019

Wu, H., Cai, A., Xing, T., Huai, S., Zhu, P., Xu, M., & Lu, C. (2021), Fertilization enhances mineralization of soil carbon and nitrogen pools by regulating the bacterial community and biomass. *Journal of Soils and Sediments*, 1-11. doi: 10.1007/s11368-020-02865-z

Wu, X., Fang, H., Zhao, L., Wu, T., Li, R., Ren, Z., et al. (2014), Mineralisation and changes in the fractions of soil organic matter in soils of the permafrost region, Qinghai-Tibet plateau, china. *Permafrost and Periglacial Processes*, *25*(1), 35-44. doi: https://doi.org/10.1002/ppp.1796

Wu, X. B., Nan, Z. T., Zhao, S. P., Zhao, L., & Cheng, G. D. (2018), Spatial modeling of permafrost distribution and properties on the Qinghai-Tibet plateau. *Permafrost and Periglacial Processes*, *29*(2), 86-99. doi: 10.1002/ppp.1971

Xu, R., Prentice, I. C., Spahni, R., & Niu, H. S. (2012), Modelling terrestrial nitrous oxide emissions and implications for climate feedback. *New Phytologist*, *196*(2), 472-488. doi: 10.1111/j.1469-8137.2012.04269.x

Yan, L., Zhou, G. S., Wang, Y. H., Hu, T. Y., & Sui, X. H. (2015), The spatial and temporal dynamics of carbon budget in the alpine grasslands on the Qinghai-Tibetan plateau using the terrestrial ecosystem model. *Journal of Cleaner Production*, *107*, 195-201. doi: https://doi.org/10.1016/j.jclepro.2015.04.140

Yang, G. B., Peng, Y. F., Marushchak, M. E., Chen, Y. L., Wang, G. Q., Li, F., et al. (2018), Magnitude and pathways of increased nitrous oxide emissions from uplands following permafrost thaw. *Environmental Science & Technology*, *52*(16), 9162-9169. doi: 10.1021/acs.est.8b02271

Yang, Y., Fang, J., Ji, C., & Han, W. (2009), Above- and belowground biomass allocation in Tibetan grasslands. *Journal of Vegetation Science*, *20*(1), 177-184. doi: https://doi.org/10.1111/j.1654-1103.2009.05566.x

Yi, S., Wang, X., Qin, Y., Xiang, B., & Ding, Y. (2014), Responses of alpine grassland on Qinghai–Tibetan plateau to climate warming and permafrost degradation: A modeling perspective. *Environmental Research Letters*, *9*(7), 074014. doi: 10.1088/1748-9326/9/7/074014

Zhang, Y., Qi, W., Zhou, C., Ding, M., Liu, L., Gao, J., et al. (2014), Spatial and temporal variability in the net primary production of alpine grassland on the Tibetan plateau since 1982. *Journal of Geographical Sciences*, *24*(2), 269-287. doi: 10.1007/s11442-014-1087-1

Zhang, Y., Zhang, N., Yin, J., Zhao, Y., Yang, F., Jiang, Z., et al. (2020), Simulated warming enhances the responses of microbial n transformations to reactive n input in a Tibetan alpine meadow. *Environment International*, *141*, 105795. doi: https://doi.org/10.1016/j.envint.2020.105795

Zhao, J., Luo, T., Wei, H., Deng, Z., Li, X., Li, R., & Tang, Y. (2019), Increased precipitation offsets the negative effect of warming on plant biomass and ecosystem respiration in a Tibetan alpine steppe. *Agricultural and Forest Meteorology*, *279*, 107761. doi: https://doi.org/10.1016/j.agrformet.2019.107761

Zhao, L., Wu, X. D., Wang, Z. W., Sheng, Y., Fang, H. B., Zhao, Y. H., et al. (2018), Soil organic carbon and total nitrogen pools in permafrost zones of the Qinghai-Tibetan plateau. *Scientific Reports*, *8*, 1-9. doi: 10.1038/s41598-018-22024-2

Zheng, Z. T., Zhu, W. Q., & Zhang, Y. J. (2020), Seasonally and spatially varied controls of climatic factors on net primary productivity in alpine grasslands on the Tibetan plateau. *Global Ecology and Conservation*, *21*, e00814. doi: 10.1016/j.gecco.2019.e00814

Zhuang, Q., He, J., Lu, Y., Ji, L., Xiao, J., & Luo, T. (2010), Carbon dynamics of terrestrial ecosystems on the Tibetan plateau during the 20th century: An analysis with a process-based biogeochemical model. *Global Ecology and Biogeography*, *19*(5), 649-662. doi: 10.1111/j.1466-8238.2010.00559.x

Zhuang, Q., McGuire, A. D., Melillo, J. M., Clein, J. S., Dargaville, R. J., Kicklighter, D. W., et al. (2011), Carbon cycling in extratropical terrestrial ecosystems of the northern hemisphere during the 20th century: A modeling analysis of the influences of soil thermal dynamics. *Tellus B: Chemical and Physical Meteorology*, *55*(3), 751-776. doi: 10.3402/tellusb.v55i3.16368

Zhuang, Q., McGuire, A. D., O'Neill, K. P., Harden, J. W., Romanovsky, V. E., & Yarie, J. (2002), Modeling soil thermal and carbon dynamics of a fire chrono sequence in interior Alaska. *Journal of Geophysical Research: Atmospheres*, *107*(D1), FFR 3-1-FFR 3-26. doi: https://doi.org/10.1029/2001JD001244

Zhuang, Q., Romanovsky, V. E., & McGuire, A. D. (2001), Incorporation of a permafrost model into a large-scale ecosystem model: Evaluation of temporal and spatial scaling issues in simulating soil thermal dynamics. *Journal of Geophysical Research: Atmospheres*, *106*(D24), 33649-33670. doi: 10.1029/2001jd900151